

## Enhanced Ionic Conductivity of Fluoride-Doped $\text{LiTi}_2(\text{PO}_4)_3$ as Solid Electrolyte of Lithium-Ion Battery

Muhammad Rizal Afif<sup>1,a</sup>, Vania Mitha Pratiwi<sup>2,b</sup>, Lukman Noerochim<sup>3,c\*</sup>

<sup>1</sup>Department of Materials and Metallurgical Engineering, Sepuluh Nopember Institute of Technology, Surabaya 60111, Indonesia

<sup>2</sup>Department of Materials and Metallurgical Engineering, Sepuluh Nopember Institute of Technology, Surabaya 60111, Indonesia

<sup>3</sup>Department of Materials and Metallurgical Engineering, Sepuluh Nopember Institute of Technology, Surabaya 60111, Indonesia

<sup>a</sup>rizalapip@gmail.com, <sup>b</sup>vaniamithapratiwi@gmail.com, <sup>c</sup>lukman@mat-eng.its.ac.id

**Keywords:** Fluoride,  $\text{LiTi}_2(\text{PO}_4)_3$ , solid-state method, conductivity, lithium-ion battery

**Abstract.** In this study,  $\text{LiTi}_2(\text{PO}_4)_3$  (LTP) was synthesized by the addition of lithium fluoride (LiF) of 0 %, 5 %, and 10 wt. %. A wet solid-state reaction method is applied by mixing  $\text{Li}_2\text{CO}_3$ ,  $\text{TiO}_2$ , and  $\text{NH}_4\text{H}_2\text{PO}_4$  into a ball mill, then calcined at 900° C for 12 hr. XRD pattern of Fluoride-doped LTP is indexed and found in two phases. First is the Nasicon phase ( $\text{LiTi}_2(\text{PO}_4)_3$ ) with rhombohedral structure, and second, the Olivine phase ( $\text{LiTiPO}_5$ ) with orthorhombic structure at the addition of 5 % and 10 wt. % of LiF. The higher LiF decreases the cell volume while the crystallite size, particle size, and material density increase. The morphology of the Fluoride-doped LTP is increasingly homogeneous and more rectangle-shape. LTP 2, adding 10 wt. % of LiF, has high ionic conductivity at  $4.77 \cdot 10^{-4} \text{ S cm}^{-1}$  as a promising candidate material for solid-electrolyte of lithium-ion battery.

### Introduction

Nowadays, batteries are one of the most widely used energy storage technology. Lithium-ion batteries are widely used in portable electronic devices and electric vehicles. Unfortunately, lithium-ion battery is hampered by their flammable electrolyte solution component<sup>1</sup>. It is a significant problem regarding the safety of using this type of lithium battery.

Current technological developments lead to the use of lithium-ion batteries with all components in a solid state<sup>2</sup>. In particular, using solid electrolytes can improve the performance and safety of lithium-ion batteries. Ceramic oxide electrolyte is a material that has the potential as a solid electrolyte because of its high chemical stability in the environment<sup>3</sup>. Solid electrolyte type NASICON  $\text{LM}_2(\text{PO}_4)_3$  is a promising candidate because of its high ionic conductivity, stability, and low cost, especially  $\text{LiTi}_2(\text{PO}_4)_3$ <sup>4</sup>.

However, using ceramic oxide electrolytes has drawbacks in high resistivity directly proportional to the interface between the electrolyte and the electrodes and lack of electrochemical stability<sup>5</sup>. Many studies have been conducted to improve the performance of  $\text{LiTi}_2(\text{PO}_4)_3$ . Partial substitution of  $\text{Ti}^{4+}$  with trivalent elements and  $\text{P}^{5+}$  with trivalent elements has been shown to increase the lithium concentration in the solid phase<sup>6</sup>. However, high electrolyte density is only obtained at high-temperature sintering for several hours. Various sintering methods have been developed to increase the density and reduce the possibility of lithium loss in the high-temperature process<sup>7</sup>. This sintering method is challenging to perform and increases the cost of solid electrolyte preparation.

Another strategy is adding molten material to the solid electrolyte, which will reduce the loss of lithium and affect its density<sup>8</sup>. Lithium Fluoride (LiF) salt can be selected to be mixed in the manufacture of solid electrolytes because it has properties as a densifying agent<sup>9</sup>. Therefore, in this study, variations in the addition of melted Lithium Fluoride (LiF) were carried out, which could improve the performance of solid electrolytes of the type of NASICON  $\text{LiTi}_2(\text{PO}_4)_3$ .

## Experimental Procedures

### *Materials Preparation*

LiTi<sub>2</sub>(PO<sub>4</sub>)<sub>3</sub> was synthesized using the solid-state reaction method. First, Li<sub>2</sub>CO<sub>3</sub>, TiO<sub>2</sub>, and NH<sub>4</sub>H<sub>2</sub>PO<sub>4</sub> are mixed by using a ball mill with methanol as solvent. The ball-to-powder ratio is 4:1, and the ball mill speed is 400 rpm for 10 hours. Then, the precursor mixture was calcined at a temperature of 900 °C for 12 hours. The as-prepared powder is ground using a mortar. Before forming into pellets, LiTi<sub>2</sub>(PO<sub>4</sub>)<sub>3</sub> powder was mixed with LiF with variations of 0%, 5%, and 10% wt., and then formed pellets were formed using a press with a pressure of 25 MPa. The pellets were sintered to stabilize the phase at a temperature of 900 °C for 12 hours.

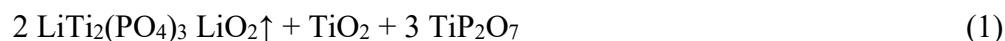
### *Electrochemical characterization*

In this study, to determine the phase formed in the sample, XRD testing was carried out using the PAN Analytical instrument with an angle range of 10°-90° with a CuKα wavelength of 1.54056 Å. For samples without the addition of LiF, prior to the XRD test, the sample was ground in the form of grinding it first using a mortar to obtain a homogeneous size. Meanwhile, samples with the addition of LiF were tested in the form of pellets. The SEM Inspect S50 machine with an energy of 20 kV was used to observe the morphological sample. Specimen preparation was carried out by grinding using a mortar and then coating the surface using AuPd to prevent charging when using SEM. The electronic conductivity test uses the EIS method with the Corrtest type CS350 Potentiostat. EIS measurements use a small AC signal of 20 mV and a DC bias voltage of more than 3V to produce a curve that can form a semi-circular arc pattern on the Nyquist Plot graph.

## Results and Discussion

The XRD characterization results showed the peak match between the synthesized LiTi<sub>2</sub>(PO<sub>4</sub>)<sub>3</sub> material with ICDD No. 00-35-0754, as shown in Fig. 1. From these results, it is also seen that other phases appear at 2θ of 24-25°, indicating that the LiTi<sub>2</sub>(PO<sub>4</sub>)<sub>3</sub> material has a high degree of crystallinity. XRD pattern shows that the diffraction peak of the sample is relatively narrow, indicating the high crystallinity of the sample. The fitting results of the XRD show the addition of LiF, causing the intensity of the peak to increase and the width of the peak to be narrower. It indicates an increase in the material's crystallinity, affecting the conductivity of the LiTi<sub>2</sub>(PO<sub>4</sub>)<sub>3</sub> sample.

The XRD pattern also shows the formation of Nasicon LiTi<sub>2</sub>(PO<sub>4</sub>)<sub>3</sub> phase with rhombohedral crystal structure in all samples. However, several peaks with low intensity are not in accordance with ICDD No. 00-35-0754. The diffraction peaks formed at angles of 18.5°, 22.4°, 27.2°, and 27.7° were identified as the peaks of TiP<sub>2</sub>O<sub>7</sub> (ICDD 00-038-1468) and TiO<sub>2</sub> (ICDD 01-083-2243) compounds. TiO<sub>2</sub> and TiP<sub>2</sub>O<sub>7</sub> compounds appeared in all samples. Based on research by Kee et al.<sup>10</sup>, the impurities in the LTP sample are formed from the decomposition reaction of LiTi<sub>2</sub>(PO<sub>4</sub>)<sub>3</sub>. It is due to the transition of Li<sub>2</sub>O into the gas phase at temperatures above 800 °C with following reaction



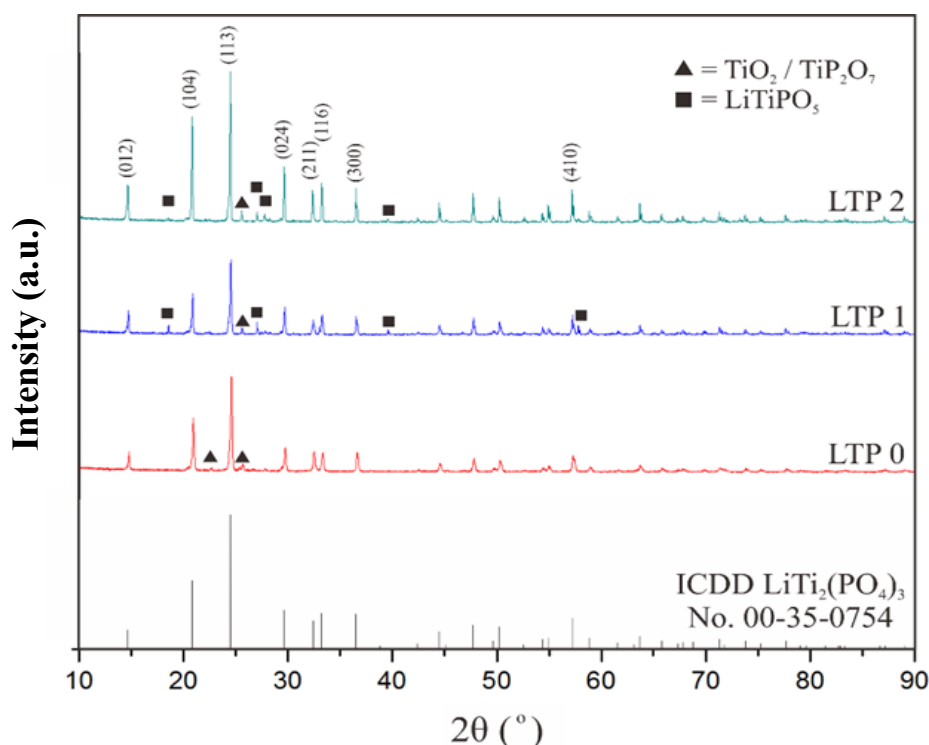


**Fig. 1.** XRD pattern of pure LTP, LTP 0, LTP 1, and LTP 2

Samples with the addition of LiF showed the emergence of another phase, namely the Olivine  $\text{LiTiPO}_5$  phase, which has an orthorhombic crystal structure. The formation of the  $\text{LiTiPO}_5$  was induced by the addition of LiF which reacted with  $\text{TiO}_2$  and  $\text{TiP}_2\text{O}_7$  impurities. The appearance of impurities in  $\text{LiTi}_2(\text{PO}_4)_3$  can be avoided using the active precursor synthesized at temperatures below  $800^\circ\text{C}$ <sup>11</sup>. At this temperature, the active precursors of  $\text{LiTi}_2(\text{PO}_4)_3$  can be formed without the appearance of  $\text{TiO}_2$  and  $\text{TiP}_2\text{O}_7$ . XRD data were also analyzed quantitatively by manual calculations and the Rietveld method using Rietica software. Analysis in the form of relative weight fraction, lattice parameter values, and crystal size. Table 1 shows the results of the phase composition formed in each sample.

**Table 1.** Percentage of Phase Composition

	$\text{LiTi}_2(\text{PO}_4)_3$ (%)	$\text{LiTiPO}_5$ (%)
<b>LTP 0</b>	100	-
<b>LTP 1</b>	89.85	10.15
<b>LTP 2</b>	74.37	25.63

Table 1 shows the percentage composition of the phase with Nasicon structure formed in all LTP samples, while the secondary phase in the form of Olivine phase was formed in samples with LiF. The lattice parameters obtained from Rietveld's analysis are shown in Table 2. The lattice parameter of  $\text{LiTi}_2(\text{PO}_4)_3$  shows a, b of 8.5129, c of 20.878, and cell volume of  $1310.31 \text{ \AA}^3$ . The increased addition of LiF decreased the size of the lattice parameters and cell volume. The decrease in cell volume indicates that there is an exchange of oxygen ions with fluoride ion where the atomic radius of fluoride ( $1.36 \text{ \AA}$ ) is smaller than the atomic radius of oxygen ( $1.40 \text{ \AA}$ )<sup>12</sup>.

**Table 2.** Comparison of lattice parameters and cell volume of  $\text{LiTi}_2(\text{PO}_4)_3$

Sample	a (Å)	b (Å)	c (Å)	V (Å <sup>3</sup> )
ICDD 00-35-0754	8.513	8.513	20.878	1310.31
LTP 0	8.513	8.513	20.875	1310.053
LTP 1	8.514	8.514	20.856	1309.109
LTP 2	8.511	8.511	20.850	1307.817

The crystal size calculation was carried out using the Debye Scherrer equation, with the results shown in Table 3. The pure LTP obtained a crystal size of 75.06 nm. In general, the addition of LiF will reduce the crystal size. With the addition of LiF of 5 wt. %, there was an increase in particle size, reaching 97.42 nm, then at the addition of 10 wt.%, it increased to 108.93 nm. This increase in crystal size will improve the mobility of lithium ions while increasing ionic conductivity<sup>13</sup>.

**Table 3.** Crystallite size  $\text{LiTi}_2(\text{PO}_4)_3$ .

Sample	Crystallite size(nm)
LTP 0	75.06
LTP 1	97.42
LTP 2	108.93

The surface morphology of the samples can be seen from the SEM characterization results in Fig. 2. All samples showed a poor rectangular particle shape with varying particle sizes. Adding LiF resulted in the size of the particle shape getting bigger and closer to a perfect rectangle. In pure  $\text{LiTi}_2(\text{PO}_4)_3$  obtained particles with a size of  $0.88\ \mu\text{m} - 12.49\ \mu\text{m}$ . The addition of LiF 5 wt.% resulted in an increase in particle size to  $1.09\ \mu\text{m} - 21.27\ \mu\text{m}$ . Meanwhile, the particle size of the sample with the addition of 10 wt. % LiF was  $3.02\ \mu\text{m} - 15.74\ \mu\text{m}$ . In the LTP 2 sample, the addition of 10 wt. % LiF has the particle size much more homogeneous than the other samples. SEM characterization also shows the porosity of the sample. All samples showed the presence of porosity. The greater the addition of LiF, the less visible porosity. It shows that adding LiF will help the particle enlargement process, reducing the grain boundaries so that the amount of porosity decreases. This condition will affect the conductivity of the material. The less porosity will increase the ionic conductivity of the material<sup>14</sup>. The reduced amount of porosity was confirmed by increasing the density of  $\text{LiTi}_2(\text{PO}_4)_3$ . The increase in material density is shown in Table 4.

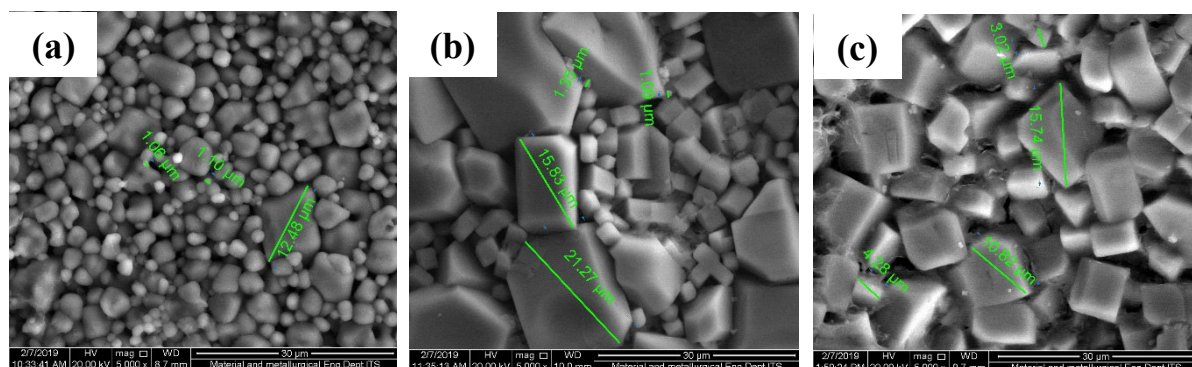


**Fig. 2.** SEM images of (a)LTP 0, (b) LTP 1, and (c) LTP 2

**Table 4.** Density of  $\text{LiTi}_2(\text{PO}_4)_3$

Sample	Density ( $\text{gr cm}^{-3}$ )
LTP 0	0.768
LTP 1	0.776
LTP 2	0.779

Measurement of the impedance of the LTP solid electrolyte sample using Electrochemical Impedance Spectroscopy (EIS). The frequency range used is 0.1 Hz - 1 MHz. Characteristics of EIS curve consist of a semicircle arc pattern (semicircle) and straight lines. Semicircle in EIS is related to the electrolyte resistance ( $R_e$ ) and charge transfer resistance ( $R_{ct}$ ). While the straight line indicates the diffusion/intercalation-de-intercalation process of lithium. The EIS test was carried out using a pellet-shaped sample with silver paste coated on both sides. The Nyquist curve plot of the EIS test results can be seen in Fig. 3. It can be seen that all samples have a single semicircle curve with different diameters. The size of the semicircle diameter shows the impedance value, the larger the diameter, the higher the impedance value, and vice versa. LTP 0 seems to have the smallest semicircle. Meanwhile, LTP 2 shows the largest semicircle diameter, indicating a large sample's

impedance value. However, it should be noted that the main property of solid electrolyte to be obtained from the EIS test is electrolyte conductivity because the increase in the size of the semicircle indicates a large change in the grain boundary impedance which is a charge transfer resistance. The value of the EIS test results is shown in Table 5.

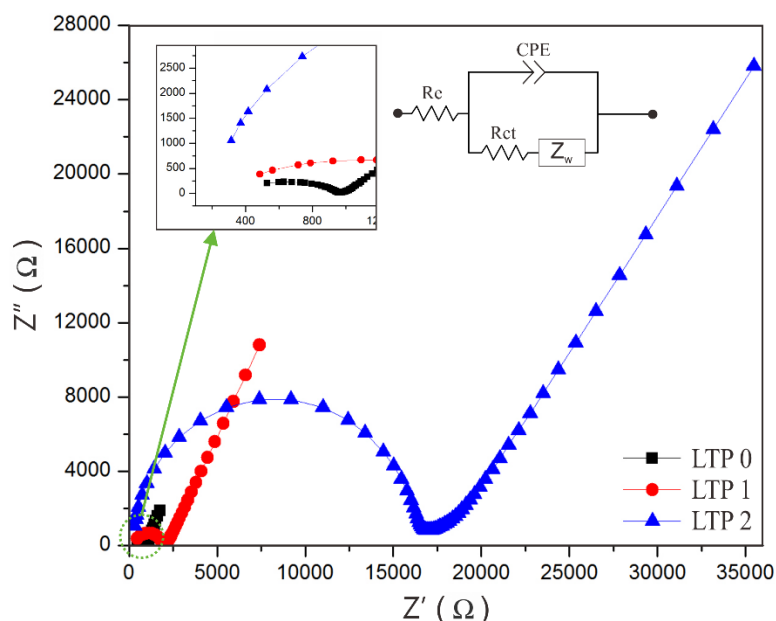


Fig. 3. Nyquist Plot of  $\text{LiTi}_2(\text{PO}_4)_3$

The addition of LiF showed the value of the electrical conductivity and total conductivity decreased. However, the total conductivity value does not indicate that this material is suitable for use as a solid electrolyte. As for electrical conductivity, adding LiF affects the material have better electrical conductivity as a solid electrolyte. Because the characteristics required by solid electrolytes are to have good ion conduction ability but low electron conduction ability to avoid short circuit in their application. This is in accordance with a study conducted by Kunshina<sup>15</sup>, on the high-frequency Nyquist curve associated with lithium ion transfer characterized by the value of electrolyte resistance and low frequency indicating grain boundary properties characterized by electronic resistance. Adding LiF enhances the solid electrolyte  $\text{LiTi}_2(\text{PO}_4)_3$  by increasing the ionic conductivity and decreasing the electrical conductivity.

Table 4. Conductivity of  $\text{LiTi}_2(\text{PO}_4)_3$

Sample	$R_e(\Omega)$	$R_{ct}(\Omega)$	$\sigma_e$ ( $10^{-6} \text{ S cm}^{-1}$ )	$\sigma_i$ ( $10^{-4} \text{ S cm}^{-1}$ )
LTP 0	346.98	601.66	188	3.26
LTP 1	303.24	1583.3	71.5	3.73
LTP 2	237.15	1562.4	7.24	4.77

It can be seen that LTP 2 has the highest ionic conductivity of  $4.77 \times 10^{-4} \text{ S cm}^{-1}$  but has the lowest electrical conductivity of  $7.24 \times 10^{-6} \text{ S cm}^{-1}$ .

## Conclusion

The solid electrolyte synthesis of lithium titanium phosphate  $\text{LiTi}_2(\text{PO}_4)_3$  using the solid-state reaction method was successfully carried out. It is found two phases formed in the sample, namely Nasicon phase ( $\text{LiTi}_2(\text{PO}_4)_3$ ) with a rhombohedral structure and a secondary phase in the form of Olivine phase ( $\text{LiTiPO}_5$ ) with an orthorhombic structure. The formation of single phase Nasicon ( $\text{LiTi}_2(\text{PO}_4)_3$ ) occurred at a concentration of 0%wt LiF. There is a second phase for the concentration of LiF of 5 wt. % and 10 wt. %, namely Olivine ( $\text{LiTiPO}_5$ ). The greater the concentration of LiF added, the increased percentage of the secondary phase formed. At the same time, the crystal size, particle size, and density of the material get bigger. The morphology of the resulting material looks

more homogeneous and is getting closer to a perfect rectangular shape, indicating an increasing crystallinity. Adding LiF improves solid electrolyte performance  $\text{LiTi}_2(\text{PO}_4)_3$ . The best performance value was obtained in the LTP 2, the addition of LiF of 10% wt, which has an ionic conductivity of  $4.77 \cdot 10^{-4} \text{ S cm}^{-1}$  but had a low electron conductivity of  $7.24 \cdot 10^{-6} \text{ S cm}^{-1}$ . It is due to phase and morphological changes after the addition of LiF.

## References

- [1] Xiong, L. *et al.* LiF assisted synthesis of  $\text{LiTi}_2(\text{PO}_4)_3$  solid electrolyte with enhanced ionic conductivity. *Solid State Ionics* 309, 22–26 (2017).
- [2] Oh, G., Hirayama, M., Kwon, O., Suzuki, K. & Kanno, R. Bulk-Type All Solid-State Batteries with 5 V Class  $\text{LiNi}_{0.5}\text{Mn}_{1.5}\text{O}_4$  Cathode and  $\text{Li}_{10}\text{GeP}_2\text{S}_{12}$  Solid Electrolyte. *Chem. Mater.* 28, 2634–2640 (2016).
- [3] Tatsumisago, M., Takano, R., Tadanaga, K. & Hayashi, A. Preparation of  $\text{Li}_3\text{BO}_3$ – $\text{Li}_2\text{SO}_4$  glass–ceramic electrolytes for all-oxide lithium batteries. *J. Power Sources* 270, 603–607 (2014).
- [4] Liang, Y., Peng, C., Kamiike, Y., Kuroda, K. & Okido, M. Gallium doped NASICON type  $\text{LiTi}_2(\text{PO}_4)_3$  thin-film grown on graphite anode as solid electrolyte for all solid state lithium batteries. *J. Alloys Compd.* 775, 1147–1155 (2019).
- [5] Inaguma, Y. *et al.* Effect of lithium isotopes on the phase transition in NASICON-type lithium-ion conductor  $\text{LiZr}_2(\text{PO}_4)_3$ . *Solid State Ionics* 321, 29–33 (2018).
- [6] Xu, X. *et al.* The preparation and lithium mobility of zinc based NASICON-type solid electrolyte  $\text{Li}_{1+2x+2y}\text{Al}_x\text{Zn}_y\text{Ti}_{2-x-y}\text{Si}_x\text{P}_{3-x}\text{O}_{12}$ . *Ceram. Int.* 40, 3819–3822 (2014).
- [7] Kosova, N. V., Devyatkina, E. T., Stepanov, A. P. & Buzlukov, A. L. Lithium conductivity and lithium diffusion in NASICON-type  $\text{Li}_{1+x}\text{Ti}_{2-x}\text{Al}_x(\text{PO}_4)_3$  ( $x=0; 0.3$ ) prepared by mechanical activation. *Ionics (Kiel)*. 14, 303–311 (2008).
- [8] Chen, K., Shen, Y., Zhang, Y., Lin, Y. & Nan, C.-W. High capacity and cyclic performance in a three-dimensional composite electrode filled with inorganic solid electrolyte. *J. Power Sources* 249, 306–310 (2014).
- [9] Kwatek, K. & Nowiński, J. L. The lithium-ion-conducting ceramic composite based on  $\text{LiTi}_2(\text{PO}_4)_3$  with addition of LiF. *Ionics (Kiel)*. 25, 41–50 (2019).
- [10] Kee, Y., Dimov, N., Minami, K. & Okada, S. Orthorhombic Lithium Titanium Phosphate as an Anode Material for Li-ion Rechargeable Battery. *Electrochim. Acta* 174, 516–520 (2015).
- [11] Kwatek, K. & Nowiński, J. L. Electrical properties of  $\text{LiTi}_2(\text{PO}_4)_3$  and  $\text{Li}_{1.3}\text{Al}_{0.3}\text{Ti}_{1.7}(\text{PO}_4)_3$  solid electrolytes containing ionic liquid. *Solid State Ionics* 302, 54–60 (2017).
- [12] Banyamin, Z. Y., Kelly, P. J., West, G. & Boardman, J. Electrical and Optical Properties of Fluorine Doped Tin Oxide Thin Films Prepared by Magnetron Sputtering. *Coatings* vol. 4 732–746 (2014).
- [13] Yu, C. *et al.* Revealing the relation between the structure, Li-ion conductivity and solid-state battery performance of the argyrodite  $\text{Li}_6\text{PS}_5\text{Br}$  solid electrolyte. *J. Mater. Chem. A* 5, 21178–21188 (2017).
- [14] Aono, H., Sugimoto, E., Sadaoka, Y., Imanaka, N. & Adachi, G. Ionic Conductivity of Solid Electrolytes Based on Lithium Titanium Phosphate. *J. Electrochem. Soc.* 137, 1023–1027 (1990).
- [15] Kunshina, G. B., Bocharova, I. V & Ivanenko, V. I. Preparation of the  $\text{Li}_{1.5}\text{Al}_{0.5}\text{Ge}_{1.5}(\text{PO}_4)_3$  solid electrolyte with high ionic conductivity. *Inorg. Mater. Appl. Res.* 8, 238–244 (2017).